Fabrication of Laser Deposited TiC/Steel Matrix Composite Coatings

W.H. Jiang, R. Kovacevic

Research Center for Advanced Manufacturing,
School of Engineering, Southern Methodist University,
1500 International Parkway, Suite #100, Richardson, TX 75081, USA
Reviewed, accepted August 25, 2003

Abstract

The present work investigates the effect of laser scanning beam speeds and the content of TiC in injected powder on morphologies and microstructures of laser deposited beads of a TiC/H13 tool steel composite. The results show that the beam scanning speeds affect the size and morphology of the beads. During laser processing, TiC melts, decomposes, and subsequently, a number of fine TiC precipitates form during cooling that are uniformly distributed in the tool steel matrix. The beam scanning speeds and the amount of injected TiC exert a strong influence on the morphology and size of the fine TiC precipitates. It is believed that the precipitated TiC is the primary phase in hypereutectic Fe-TiC. Rapid cooling develops martensite with retained austenite in a steel matrix. The precipitated TiC can refine grains of the steel matrix as a solidified nucleus. TiC/H13 tool steel composite coatings with various contents of TiC were produced using the laser deposition processing technique.

Introduction

Laser cladding is widely used for creating various surface coatings of a significant thickness that can effectively protect substrates from harsh service conditions. Various coating materials, such as carbides, oxides, nitrides, borides and their composites, have been developed [1-4]. These coatings display high hardness, wear, erosion and corrosion resistance, heat insulation.

Metal matrix composites (MMCs) as coatings have recently attracted much interest, for they combine excellent ductility and toughness of metallic matrices with high strength and hardness of ceramic reinforcements. Due to its high hardness, melting point, and thermodynamic stability as well as availability, TiC is extensively used as a reinforcing phase in MMCs' coatings, such as Ni based [5-8] and steel based composites [8-10]. Due to a relatively low cost, iron and steels as a coating matrix have a potential application prospect. Utilizing laser surface alloying, Ariely et al. [8] produced TiC reinforced steel coatings on the surfaces of Armco iron, AlSl 1045 and 1095 steels, exhibiting a higher hardness. Tassin et al. [9] incorporated TiC into the surface of AlSl 316 L stainless steel by laser processing, which substantially improved sliding wear resistance. Jiang and Molian [10] increased life of die-casting dies by laser surface processing with micrometer- and nanometer-sized TiC powder.

Slurry erosion happens extensively in the industries of mining, metallurgy, and crude-oil drilling, etc. Materials with improved wear resistance to slurry erosion are in increasing demand in the industries. It is well known that hard materials have a high erosion resistance at a low impact angle, while ductile materials have a high erosion resistance at a high impact angle.

However, in some service conditions, components suffer slurry erosion at varying impact angles. Therefore, it is of practical significance to develop coatings with an overall excellent erosion resistance, no mater what the impact angles are. Considering their good combination of hardness and ductility, steel matrix composites may be potential erosion resistant materials at various impact angles. Utilizing laser surface processing, the present work tries to develop TiC/H13 tool steel composite coatings as a new erosion resistant material.

Laser processing is characterized by its high energy density, low heat input, and consequently, high heating and cooling rates that minimizes its effect on a substrate. However, laser processing parameters such as beam power and beam scanning speed affect metallurgical quality, microstructures, and furthermore, mechanical properties of coatings [10]. In this work, laser deposition is used to synthesize TiC/H13 tool steel coatings with different concentrations of TiC. The effect of beam scanning speeds on the microstructures of coatings is investigated for a given laser beam power and powder feeding rate. Their erosion resistance is being investigated and will be reported.

Experimental procedure

Fig. 1 shows the schematic diagram of the 3D laser cladding system setup used in this investigation. A 1 kW continuous wave Nd: YAG laser with a 200-mm focusing optics is used to deposit the powders. The laser beam guided by the optical fiber is reflected from the partial reflective mirror, and is focused on the substrate by the set of lens arranged in the laser head. The computer-controlled powder feeders are used for dosing and feeding the powder mixture into the desired composition, and allow for an exact setting and continuous change of the powder mixture during the cladding process [11]. The alignment of the laser beam, powder nozzles, and their positioning in relation to the substrate must be accurate for the process to be reproducible. The feeding rate of each of the powders and laser processing parameters are controlled automatically.

AISI 4140 steel plate was used as a substrate, whose composition is shown in Table 1. H13 tool steel powder was used as a matrix of composite coatings. The original size of the H13 tool steel powder is around 50-100 μm. Its composition is also shown in Table 1. The original TiC particles are 50-100 μm.

Table 1 Nominal chemical composition of steels used, wt.%

Element	C	Cr	Mo	Mn	Si	V	Fe
4140	0.4	1.0	0.2	0.9	0.2	-	Balance
H13	0.4	5.0	1.0	0.4	1.1	1.1	Balance

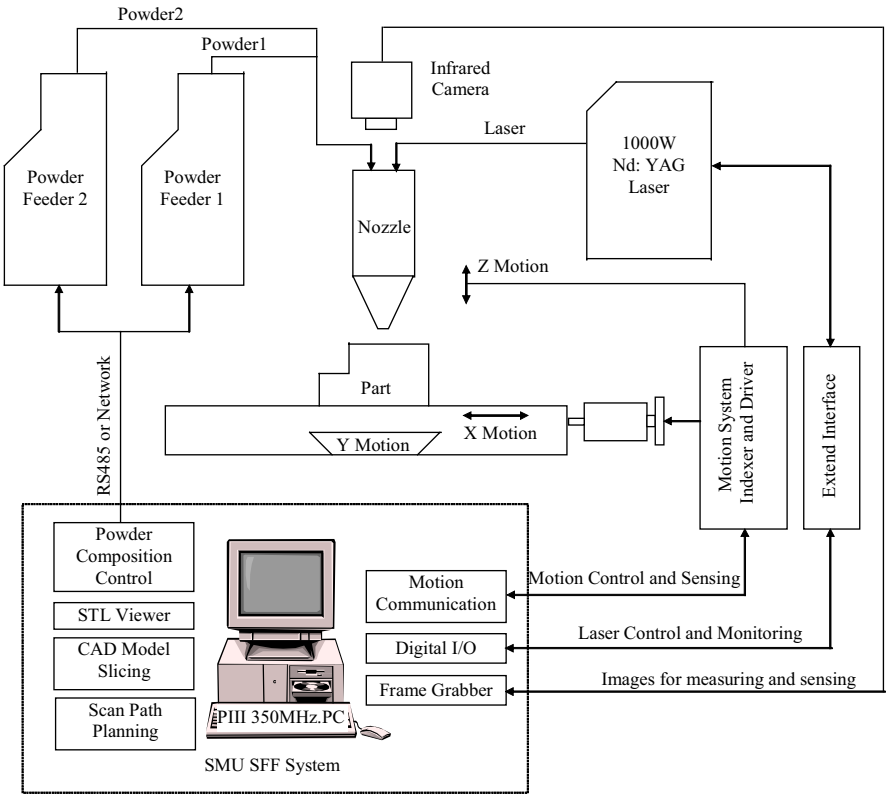

Fig. 1 Schematic diagram of 3D laser cladding system setup.

The laser beam power used in the experiments was 380 W, with a spot diameter of 1 mm. The beam scanning speeds were set to 5.08, 7.62, 10.16, and 12.7 mm s^{-1}. A feeding system was used for direct injection of powders with argon flow as a powder carrier. The TiC and H13 tool steel powder was injected by a powder feeder through four nozzles of 1 mm in diameter. The feeding rates of TiC and H13 tool steel are dependent on designed constitutions of coatings. They are (3 × TiC vol.%) g min^{-1} and (4.65×H13 vol.%) g min^{-1} for TiC and H13 tool steel, respectively. Single and double layer beads were deposited at various beam scanning speeds. In case of overall coating, substrate samples (25.4 mm × 25.4 mm) were coated uniformly with double layers of about 1 mm in thickness. The beam scanning speed is 10.16 mm s^{-1}. A 40% overlap of a successive melting track was selected to produce a uniform coating on a substrate.

The transverse cross sections of the deposited beads were cut for microstructural examination. The optical microscopy and electron microprobe with energy dispersive analysis of X-ray (EDAX) were used for microstructural observation and microanalysis of composition. X-ray diffraction with Cu Kα was performed to identify the phases in coatings.

Results

Laser beam scanning speeds affect the sizes and morphologies of deposited beads. However, their effect is independent of the constitutions of the deposited powder, that is, the proportion of H13 tool steel to TiC. The typical morphologies of the cross sections of the beads

produced at various beam scanning speeds are shown in Fig. 2. It is well known that a laser clad layer can be divided into three zones, i.e., coating, melting and heat-affected zones in a substrate. From Fig. 2, it can be seen that coating and melting zones are influenced severely by the beam scanning speeds. The faster the beam moves, the smaller the volume and the mass of the coatings. Yet, the melting zone of the substrate decreases with decreasing beam scanning speed, and disappears completely at the minimal speed, i.e. 5.08 mm s^{-1}. It can be seen that only two intermediate beam scanning speeds can develop well geometric and symmetric beads. At the maximum beam scanning speed, 12.7 mm s^{-1}, the coating fails to coincide with the melting zone; while at the minimal speed, the coating tends to lean. It is noted that the maximum beam scanning speed leads to involvement of the substrate material into the coating, but fails to homogenize them, as shown in Fig. 2d. This may result from both the larger melting zone in the substrate and higher solidification rate, which mixed much substrate material with deposited materials. Double layer depositions have the same melting and heat affected zones as the single ones. Undoubtedly, a double layer deposition increases the sizes of deposited coatings. Worthy to mention, the beads of the double layer depositions at the minimal beam scanning speed completely lose geometrical symmetry.

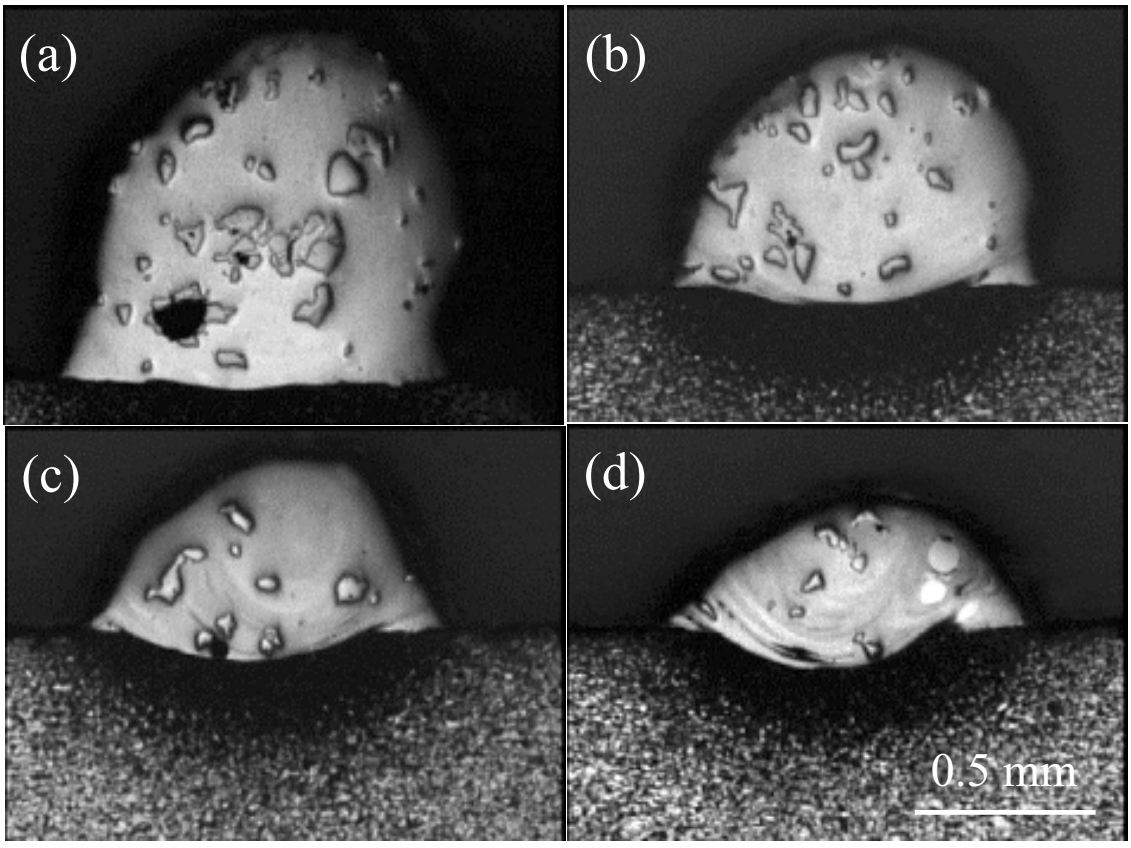

Fig. 2 Morphologies of beads of 60 vol.% TiC/H13 steel formed by single layer scanning at speeds of (a) 5.08, (b) 7.62, (c) 10.16 and (d) 12.7 mm s^{-1}.

From Fig. 2, it can be seen that the interface morphologies between a melting zone and a heat-affected zone change with the beam scanning speeds. By decreasing the beam scanning speeds, their curvatures decrease. In the example of the minimal beam scanning speed, a melting zone disappears and the interface becomes planar. Fig. 3 shows the typical high magnification micrographs of planar (at a speed of 5.08 mm s^{-1}) and curved (at a speed of 12.7 mm s^{-1}) interfaces. Evidently, the curved interface has a better melting bond than the planar.

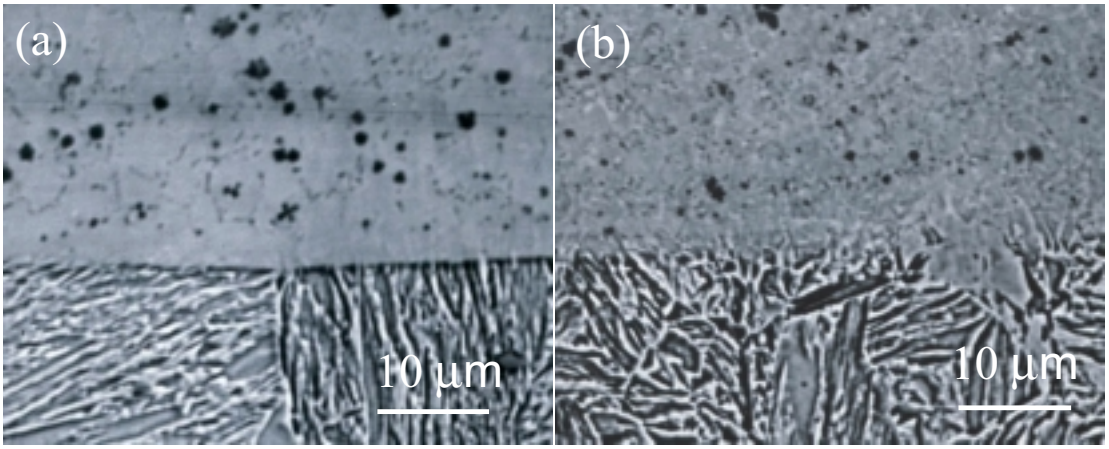

Fig. 3 High magnification micrographs of interfaces in 60 vol.% TiC/H13 steel formed by single layer scanning at speeds of (a) 5.08 and (b) 12.7 mm s^{-1}.

High magnification observation indicates that TiC particles decompose, and a great number of fine precipitates formed during laser processing. For this reason, the injected coarse TiC particles in beads appear fewer in the low magnification micrographs (Fig. 2). By increasing the beam scanning speeds, the fine precipitates decrease. Fig. 4 shows the typical microstructures of the beads produced at various beam scanning speeds.

For all the coatings, the fine precipitates are well distributed in steel matrices. Fig. 5 shows the backscattered electron images of the beads with 40, 60, and 80 vol.% TiC formed at a beam scanning speed of 10.16 mm s^{-1}. In these images, both the coarse TiC and the fine precipitates appear dark, indicating that their constituting elements are lighter than the iron matrix. EDAX demonstrated that fine precipitates are rich in Ti. Furthermore, it can be seen that by increasing the contents of the injected TiC, the fine precipitates increase both in quantity and size. The injected TiC particles exhibit clear, smooth edges and no reaction layer, indicating that they melt and dissolve rather than react with the melt during laser processing.

The morphologies and sizes of the fine precipitates are related to the contents of the injected TiC. Fig. 6 shows the fine precipitates in the beads with various contents of injected TiC produced at a beam scanning speed of 10.16 mm/s. In 40 vol.% TiC, they assume substantially spherical and cubic shapes. In 60 vol.% TiC, some precipitates evolve into small flower-petal shapes, while the majority are still spherical. But, in 80 vol.% TiC, the precipitates are rather large and take spherical, cross, rod, and dendrite forms.

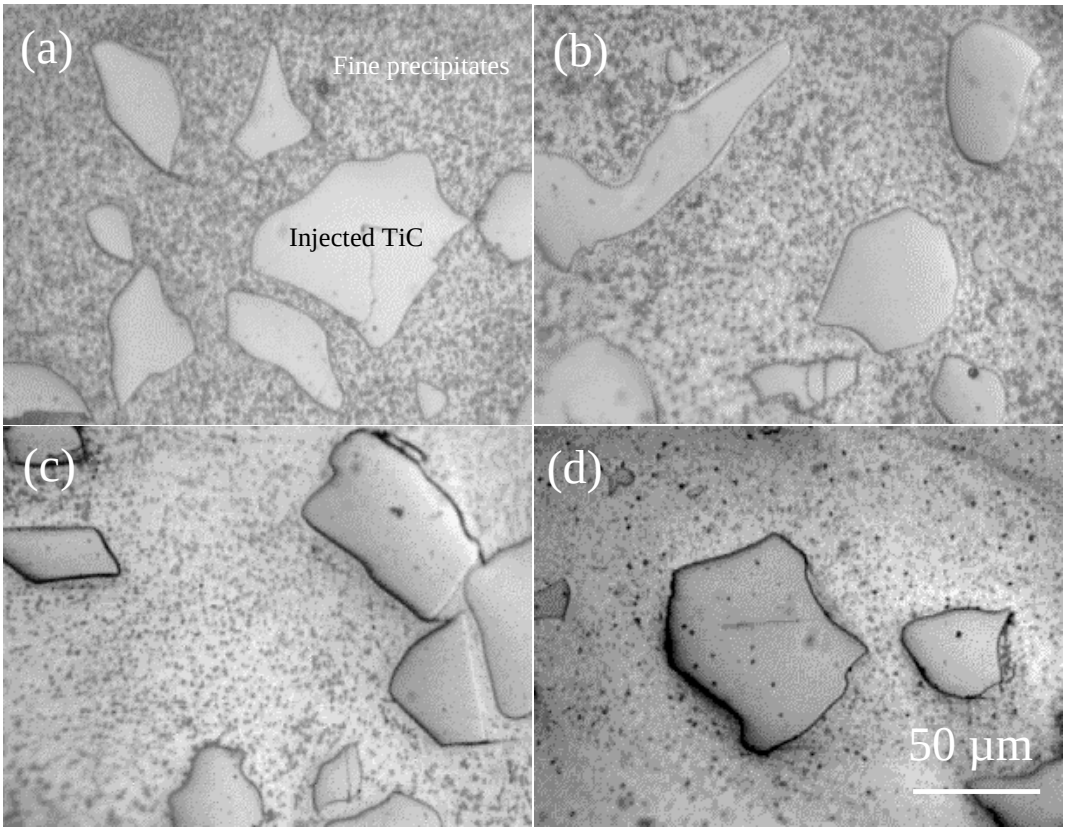

Fig. 4 Microstructures of 60 vol.% TiC/H13 steel formed by single layer scanning at speeds of (a) 5.08, (b) 7.62, (c) 10.16 and (d) 12.7 mm s^{-1}.

By a careful examination of Fig. 6b, it can be found that numerous fine precipitates are located at the center of the matrix grains. This indicates that they acted as a heterogeneous site for solidified nucleus of steel matrix grains to nucleate.

X-ray diffraction analysis was performed on the coatings with 40, 60, and 80 vol.% TiC produced at the beam scanning speed of 10.16 mm s^{-1}, respectively. The resulting diffraction patterns are shown in Fig. 7. It can be seen that the diffraction patterns of all the coatings are similar, and there are only diffraction peaks of steel matrix and TiC, indicating that TiC is only the secondary phase. These results mean that the fine precipitates are also TiC. The steel matrices are martensite and retained austenite.

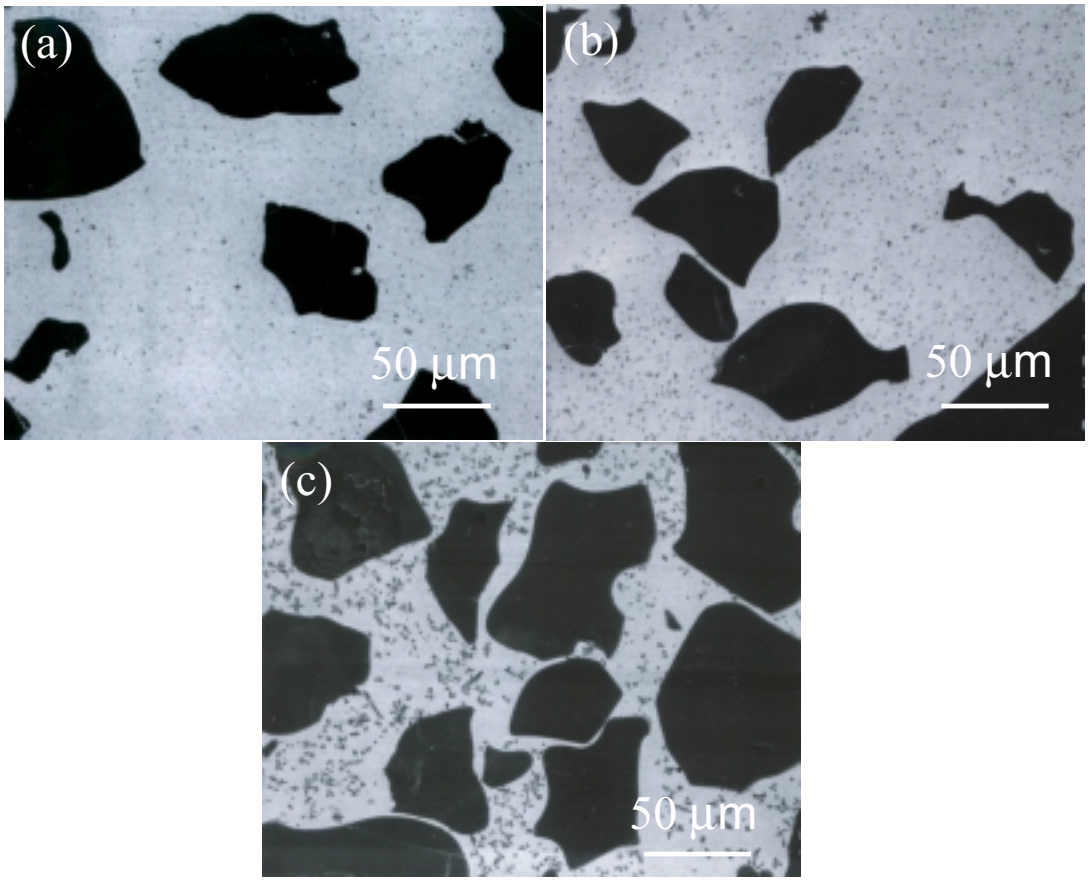

Fig. 5 Backscattered electron images (BEI) of (a) 40, (b) 60 and (c) 80 vol.% TiC/H13 steel formed at a beam scanning speed of 10.16 mm s^{-1}.

Discussion

The present results demonstrate that sizes and morphologies of the deposited beads are closely related to a beam scanning speed. In fact, they are dependent on the proportion of a powder feeding rate to a beam speed for a given powder constituent. During laser processing, laser energy is absorbed by both fed powder and substrate. Undoubtedly, their proportion decides the morphologies of the beads. Changing a beam speed is equal to inversely modifying a powder feeding rate. In the case of a smaller powder feeding rate, or a larger beam scanning speed, the amount of powder injected per unit time is small. Consequently, the energy that the powder absorbs is smaller, and the more energy may be spent to melt a substrate, resulting in a larger melting zone and a smaller bead. That is obvious for the maximum beam scanning speed (12.7 mm s^{-1}) used in the work (Fig. 2d). In the case of a larger powder feeding rate, or a lower beam scanning speed, more powder is injected. Therefore, more energy is absorbed by the injecting powder than the substrate. That results in a larger bead and a smaller melting zone. The situation of the minimal beam scanning speed (5.08 mm s^{-1}) is typical (Fig. 2a). Furthermore, no obvious

melting bond at the interface (at a speed of 5.08 mm s^{-1}) (Fig. 3a) can be explained in this viewpoint.

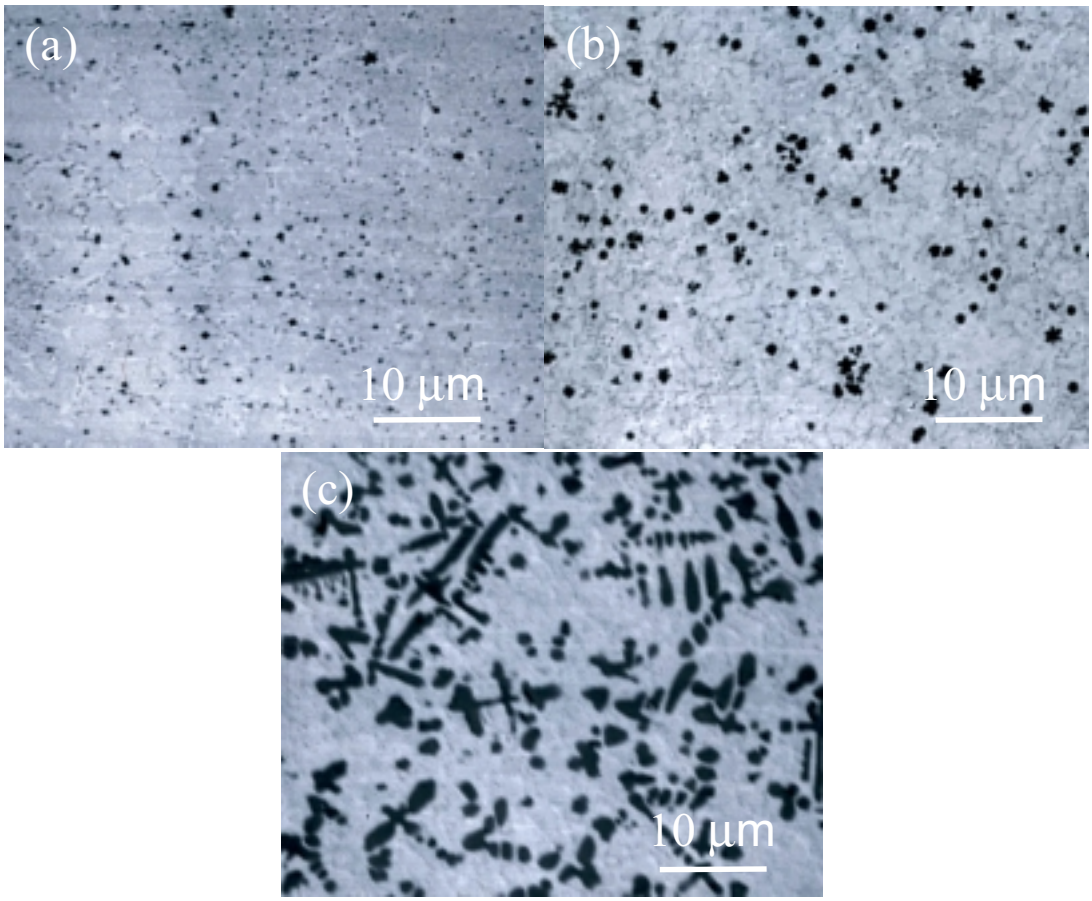

Fig. 6 High magnification BEI of (a) 40, (b) 60 and (c) 80 vol.% TiC/H13 steel formed at a beam scanning speed of 10.16 mm s^{-1}.

At the minimal beam scanning speed, the lack of a melting zone in a substrate results in a weak interface bond between the coating and substrate, as shown in Fig. 3a. Evidently, this speed is not suitable for producing a coating, not to mention the asymmetrical bead it produced (Fig. 2a and Fig. 3), that may accommodate gas and cause formation of pores during overlapping in coating production. However, the maximum beam scanning speed fails to make the upper coating coincide properly with the lower melting zone. More severely, some substrate material in the melting zone does not mix well with the deposited materials (Fig. 2d). These disadvantages make it unsuitable for producing a coating. In view of the morphology of beads, both the maximum and minimal beam scanning speeds are not ideal for coating production, while the intermediate beam scanning speeds, 7.62 and 10.16 mm s^{-1} seem to be appropriate.

The smooth edges of the coarse TiC particles indicate that the injected TiC melts and dissolves rather than reacts with the melt. As it is well known, the laser beam is characterized by a high energy density. The degree of absorption of the laser beam on metal and ceramic is very different. Ceramics have a much higher capability to absorb laser energy than metals [12].

Therefore, in spite of its extremely high melting point (3140^{o}C) [13], melting of TiC occurs during processing. As the laser processing time is extremely short, its melting is incomplete and unmelted TiC remains.

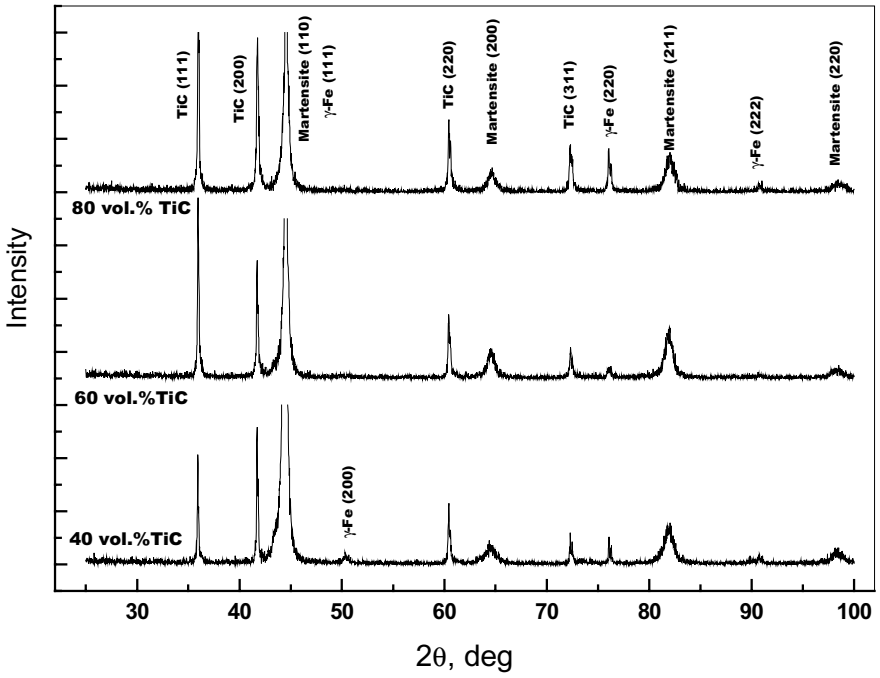

Fig. 7 X-ray diffractogram of 40, 60, 80 vol.%TiC/H13 tool steel formed at a beam scanning speed of 10.16 mm s^{-1}.

As melted TiC has a high tendency to dissociate into Ti and C, melting of a large amount of TiC results in a substantial increase in the concentration of Ti and C in the melt. Undoubtedly, TiC reprecipitate in the melt during cooling. EDAX and X-ray diffraction analysis confirms that fine TiC reprecipitated during subsequent cooling may contain less amount of other carbide forming elements, such as Mo and Cr. As the melt cools at a relatively high rate, solidified structures must be in a thermodynamic nonequilibium. That results in the development of various morphologies of TiC. At a higher beam speed and a lower content of injected TiC, the TiC precipitated in globular and cubic shapes. By lowering the beam scanning speed and increasing the amount of injected TiC, they tend to assume hexagonal and flower-petal shapes and finally the form of dendrites. This shows that the morphologies of TiC are closely related to the processing parameter and composition of melts. Considering the high contents of injected TiC, other alloying elements in the melt are neglected. The melt is approximately taken as the binary components of Fe and TiC. Refer to the binary Fe-TiC phase diagram (Fig. 8) [14], we explain qualitatively the morphologies of TiC. It can be seen that all the present constitutions of the coatings are hypereutectic. Therefore, TiC precipitates as a primary phase during cooling. Their morphologies depend on growth, as their nuclei are globular. Various morphologies of TiC can be developed during growth [15]. At a lower beam speed, solidification lasts a longer time and

primary TiC has time to grow a bit. For a higher content of injected TiC, the melt has a higher concentration of Ti and C, that is, a higher supersaturation. Therefore, their growth rate is higher, as a high solute concentration speeds up growth. Observed morphologies of TiC, spherical, faceted, rod, flower-petal shapes, and dendrites are from various growth stages. Due to rapid solidification, it is believed that the deposited beads are far from equilibrium and precipitated TiC is only primary phase during solidification.

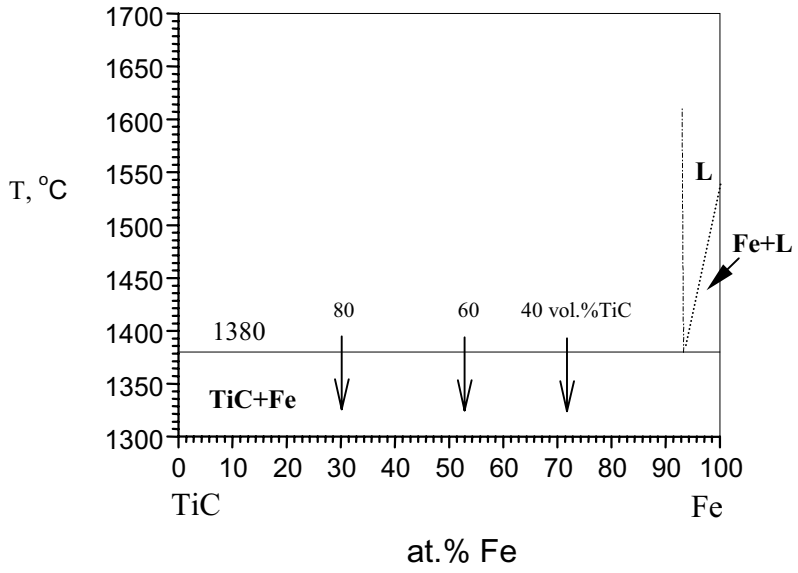

Fig. 8 Fe-TiC phase diagram [14].

In all the coatings, fine TiC precipitates are uniformly distributed in the matrix. They do not segregate around coarse TiC particles. This indicates that titanium and carbon atoms released by injected TiC are well distributed in melts. Their homogeneous distribution must be attributed to vigorous convection caused by rapid heating of the laser beam. A convective trace is evidenced in Fig. 2. It seems that the larger the beam scanning speed, the more obvious the convection.

Rapid cooling leads to the transformation of steel matrices into martensite (Fig. 7) that hardens a steel matrix. The fine precipitated TiC was observed to be a solidified nucleus for the steel matrix (Fig. 6b). They refined the grain structures of the matrix. In fact, it is well known that TiC is a good refiner for steels. Undoubtedly, this favors to modify solidified structures and furthermore, to improve both the strength and toughness of the steel matrix.

The present work indicates that microstructures of deposited beads are closely related to processing parameters. The beads with microstructures of coarse injected and fine precipitated TiC are developed. It is believed that tailored microstructures of TiC/H13 steel composite coatings can be achieved by choosing appropriate laser processing parameters.

As well known, fine particles would improve the mechanical properties of composites. It is expected that melting of coarse TiC and subsequent reprecipitation of fine TiC would impart better overall mechanical properties to coatings than the mechanical insertion of coarse TiC particles. Both the coarse remaining and the fine precipitated TiC particles are believed to have a clean interface with the steel matrix, as the original surface of injected TiC melts, a fresh surface is developed, and fine TiC precipitates are formed in-situ within the melts. Therefore, a stronger interface bond between TiC and the matrix may be achieved. As well known, the interface is a crucial location affecting the mechanical properties of composites. Impurity atoms usually tend to adhere to the surfaces of particles that disfavor an interface bond. In-situ formed composites can circumvent such disadvantages and therefore, have received much attention recently [16]. It is believed that the interface quality between TiC and the matrix in the present coatings is the same as that in in-situ formed composites. It is expected that the coating composites possess better overall mechanical properties.

Conclusions

1. The beam scanning speed affects the size and morphology of the deposited beads. The faster the beam moves, the larger the melting zone at the substrate, and the smaller the deposited zone. But, the size of heat-affected zones is independent on beam scanning speed.
2. The higher beam scanning speed fails to mix the deposited material properly with a substrate.
3. During laser processing, TiC melts, decomposes, and subsequently, a number of fine TiC precipitates form. They are uniformly distributed in the steel matrix, which is attributed to vigorous convection caused by rapid heating.
4. The beam scanning speeds and the amount of injected TiC have a remarkable impact on the morphology and size of the precipitated TiC. The lower the beam scanning speeds and the more the injected TiC, the larger the precipitated TiC. The larger TiC assumes spherical, rod, flower-petal, and dendrite shapes, while the smaller TiC is spherical and faceted.
5. It is believed that precipitated TiC is the primary phase in hypereutectic Fe-TiC.
6. Steel matrices in coatings are martensite with retained austenite. Precipitated TiC can refine grains of the steel matrix as a solidified nucleus.

Acknowledgements

The authors would like to express gratitude to Dr. H. H. Mei, Mr. Z.G. Liu and Mr. M. Valant for their helps during the experimental work.

References

1. T.C. Lei, J.H. Ouyang, Y.T. Pei and Y. Zhou, Surface Engineering, 12, 1996, 55.
2. B.J. Kooi, Y.T. Pei and J.Th.M. De Hosson, Acta Mater., 51, 2003, 831.
3. A. Agardwal, Surface Engineering, 17, 2001, 66.
4. Y.T. Pei, J.H. Ouyang and T.C. Lei, Surface and Coating Technology, 81, 1996, 131.
5. Y. T. Pei and T.C. Zou, Mater. Sci. Eng. A, A241, 1998, 259.
6. Q. Li, T.C. Lei and W.Z. Chen, Surface and Coating Technology, 114, 1999, 278.
7. J.H. Ouyang, Y.T. Pei, T.C. Lei and Y. Zhou, Wear, 185, 1995, 167.

8. S. Ariely, M. Bamberger, H. Hugel and M. Geller, SPIE Vol. 1972, 8th Meeting on Optical Engineering in Israel, 1992, 284-292.
9. C. Tassin, F. Laroudie, M. Pons and L. Lelait, Surface and Coating Technology, 76-77, 1995, 450-455.
10. M. Riabkina-Fishman, E. Rabkin, P. Levin, N. Frage, M. P. Dariel, A. Weisheit, R. Galun and B.L. Mordike, Mater. Sci. Eng. A, A302, 2001, 106.
11. R. Kovacevic, D. Hu, and M. Valant, "Apparatus and Method for Controlling the multiple Metal/Ceramic powder Feeding Systems", (Invention Disclosure, submitted to Southern Methodist University), May 2002.
12. To Hoon Kim, Section A-ICALEO (the International Congress on Applications of Lasers and Electro-Optics), Laser Institute of America: 1997, 21.
13. Wenping Jiang and Pal Molian, Surface and Coating Technology, 135, 2001, 139.
14. P. Villars, A. Pronce and H. Okamoto, in "Handbook of Ternary Alloy Phase Diagrams" (ASM International, 1995) p. 6850.
15. W.H. Jiang, W.D. Pan, G.H. Song and X.L. Han, J. Mater. Sci. Lett., 16, 1997, 1830.
16. H. Berns and B. Wewers, Wear, 250-251, 2001, 1386.